第 50 卷 第 7 期/2023 年 4 月/中国激光 研究论文

中国激光

瓦级高效率中红外全固态3.8 μm连续波Fe∶ZnSe激光器

沈炎龙*，万颖超，汪由胜，李高鹏，马连英，柴童星，陈正阁，朱峰，黄珂，冯国斌
西北核技术研究所激光与物质相互作用国家重点实验室，陕西 西安 710024

摘要 报道了瓦级高效率中红外3.8 μm连续波全固态激光器。采用自行研制的波长为2.8 μm的光纤激光器泵浦Fe∶ZnSe晶体，并通过液氮对晶体进行制冷，获得了中心波长为3.8 μm的连续激光输出。激光器的最大输出功率为0.97 W，斜率效率达到38.6%，泵浦阈值约为0.4 W。

关键词 激光器；全固态激光器；中红外激光；Fe∶ZnSe晶体；高效率
中图分类号 TN212；TN248.1 **文献标志码** A **DOI**：10.3788/CJL221087

1 引 言

中红外3～5 μm波段处于大气传输窗口，工作在此波段的激光源在激光医疗、红外泵浦、光谱学以及红外对抗等领域有着十分广阔的应用前景，并已成为国内外研究热点[1-4]。目前，产生此波段激光输出的方法主要有线性方法和非线性方法两大类，其中线性方法是基于增益介质直接振荡产生中红外激光输出，无非线性频率变换过程，主要包括DF激光器[5]，中红外光纤激光器[6-7]，半导体量子级联激光器[8]，中红外Fe∶ZnSe激光器[1,9]，充有C_2H_2[10]、HBr[11]或CO_2的空芯光纤气体激光器[12]等；非线性方法是基于特殊晶体的非线性效应实现对泵浦光的频率转换，从而获得中红外激光输出，主要包括光参量振荡(OPO)激光器[13-14]、光学差频激光器[15]以及倍频激光器[16]等。相较于其他激光器，中红外Fe∶ZnSe激光器受益于Fe∶ZnSe晶体材料超宽的吸收光谱和荧光光谱以及较大的吸收和发射截面，具有效率高、结构紧凑、稳定性好、可定标放大等优点，受到了研究者的青睐。自1999年美国研究者首次利用Fe∶ZnSe晶体获得中红外4.0～4.5 μm激光输出以来，人们掀起利用2.7～3.0 μm激光源泵浦Fe∶ZnSe晶体产生3.7～5.0 μm激光的研究热潮。在脉冲输出方面，研究者主要基于增益开关工作机制，即利用Er∶YAG脉冲激光器[17-19]、Cr∶ZnSe脉冲激光器[20]以及HF脉冲激光器[21]等泵浦Fe∶ZnSe晶体获得3.7～5.0 μm激光脉冲输出，其中最大单脉冲能量达到10.6 J[17]。同时也有基于调Q[22-23]和锁模[24]获得脉冲输出的报道。在连续输出方面，研究者主要利用连续运转的Er∶YAG激光器[25]、Cr∶ZnSe激光器[26]和中红外氟化物光纤激光器[27]等泵浦Fe∶ZnSe晶体，获得连续激光输出。2012年，Evans等[25]采用两台功率为1.5 W的Er∶YAG连续激光器作为泵浦源，获得了最大功率为840 mW的4.14 μm连续激光输出；2017年，Martyshkin等[26]利用最大功率约为23 W的Cr∶ZnSe连续激光器作为泵浦源，获得了最大输出功率为9.2 W的4.15 μm连续激光输出；2018年，Pushkin等[27]利用自制Er∶ZBLAN光纤激光器作为泵浦源，获得了最大功率为2.1 W的连续激光输出，不同输出功率下的激光器波长在4.01～4.20 μm范围内变化。可以看出，在自由运转条件下，上述报道的连续输出激光波长均在4 μm以上。

受材料和泵浦源的限制，国内基于Fe∶ZnSe晶体产生中红外激光的研究起步相对较晚，相关研究主要集中在利用3 μm波段脉冲激光泵浦Fe∶ZnSe晶体产生4～5 μm脉冲输出。2018年，孔心怡等[28]利用非链式HF激光器作为抽运源，室温下获得了最大单脉冲能量为65 mJ的4.3 μm激光输出，斜率效率为37%。2019年，Li等[29]采用脉冲重复频率为1 kHz、波长为2.9 μm的光学参量振荡器泵浦Fe∶ZnSe晶体，低温下获得了脉冲能量为63 μJ、脉宽为34.4 ns的激光输出，光光转换效率为25.2%。另外，该课题组还利用Cr∶Er∶YAG脉冲激光器作为泵浦源，获得了能量为197.6 mJ的4.0 μm激光输出[30]。2020年，Pan等[31]利用脉冲HF激光器作为泵浦源，室温下获得了脉冲能量为502 mJ的激光输出，斜率效率为32.6%，并研究了泵浦光斑尺寸对抑制横向寄生振荡的影响。相较于连续激光泵浦源，脉冲泵浦源的峰值功率比连续激光往往要大几个

收稿日期：2022-07-28；**修回日期**：2022-09-09；**录用日期**：2022-09-26；**网络首发日期**：2022-10-05
基金项目：激光与物质相互作用国家重点实验室基金(SKLLIM1911)
通信作者：*shenyanlong@nint.ac.cn

数量级，因此脉冲泵浦 Fe:ZnSe 晶体更易于实现粒子数反转，获得高增益。室温下，基于 Fe:ZnSe 晶体产生连续激光输出存在较大难度，这是因为 Fe^{2+} 的激光上能级寿命在室温下非常短（～370 ns）[20]，非常不利于形成粒子数反转条件。因此，若要获得连续输出，必须使 Fe:ZnSe 晶体工作在低温（比如 77 K，对应的激光上能级寿命为～57 μs）条件下[20]，同时，需要以 3 μm 波段连续激光光源作为泵浦源。当前国内 3 μm 波段连续激光光源尚不成熟，到目前为止，国内基于 Fe:ZnSe 晶体获得 3.7～5.0 μm 连续波激光输出的研究鲜有报道。

2014 年以来，本课题组基于氟化物光纤较为深入地开展了中红外 3 μm 波段光纤激光器研究，在国内率先实现了 10 W 级高效率单模 2.8 μm 连续激光输出[32]，并基于掺钬光纤获得了～2.9 μm 连续激光输出。本文利用自研的 2.8 μm 连续光纤激光器泵浦 Fe:ZnSe 晶体，设计了可产生 3.8 μm 连续波的全固态激光器，激光器的最大输出功率为 0.97 W，斜率效率为 38.6%。

2　实验装置

图 1 给出了中红外 Fe:ZnSe 全固态连续波（CW）激光器的结构示意图。泵浦源为自制中红外光纤激光器，采用 975 nm 半导体激光器泵浦长度约为 3.5 m 的 Er（摩尔分数为 6%）氟化物光纤（纤芯直径为 30 μm），激光器工作波长为 2.8 μm，最大连续输出功率约为 4 W。

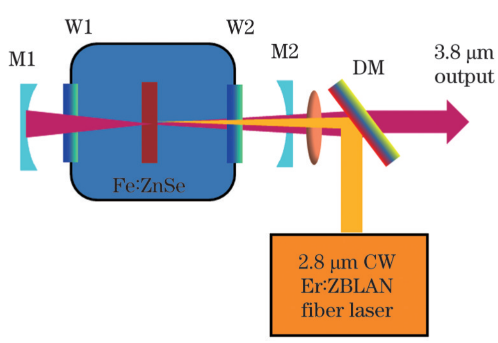

图 1　Fe:ZnSe 连续波激光器的结构示意图

Fig. 1　Structural diagram of Fe:ZnSe CW laser

增益介质为采用化学气相沉积法制备的 Fe:ZnSe 晶体，掺杂浓度约为 1.0×10^{19} cm^{-3}，厚度为 3.5 mm，截面为 10 mm×10 mm。由于晶体折射率较大（n～2.4），端面菲涅耳反射引起的损失高达 17%，不利于高效泵浦。因此，对晶体两个端面进行了光学抛光，端面平行度小于 20″，并镀制 2.7～4.8 μm 增透膜，镀膜后的晶体透过率曲线如图 2 所示。4 μm 光子跃迁发生在 Fe^{2+} 的 $^5T_2$ 和 ^5E 能级之间，ZnSe 晶体中的 Fe 离子能级间的无辐射弛豫速率随着温度的升高而增加[33]，导致上能级 $^5T_2$ 的寿命由低温（77 K）下的 57 μs 缩短至室温（300 K）下的 370 ns[20]。因此，为了获得连续激光输出，必须对晶体进行低温制冷处理[27]。实验使用的低温制冷器采用液氮作为制冷剂，温度控制范围为 77～325 K，温度精度可达 ±0.1 K。通光窗口 W1 和 W2 均为口径为 50 mm、厚度为 3 mm 的 CaF_2 平面镜片，为了尽可能降低泵浦损失，窗口镜片的两面均镀有 2.7～5.0 μm 增透膜。通过真空泵将制冷器中装载晶体的腔室抽至～0.1 Pa。谐振腔采用双凹稳定腔结构，全反镜和输出镜均为曲率半径为 50 mm 的 CaF_2 凹面镜。其中，反射镜 M1 在 3.7～4.7 μm 高反，反射率大于 99%，在 2.6～3.0 μm 高透，透过率大于 95%。输出镜 M2 在 3.7～4.7 μm 高反，反射率为 65%，在 2.6～3.0 μm 高透，透过率大于 95%。与文献[25-27]中采用的双向泵浦和前向泵浦不同，本实验设计的泵浦方式为后向端面泵浦。泵浦耦合透镜为焦距为 50 mm 的未镀膜的 CaF_2 透镜。双色镜（DM）在 3 μm 处高反，在 4 μm 处高透，采用 45°角放置，用于分离泵浦光和 4 μm 激光。

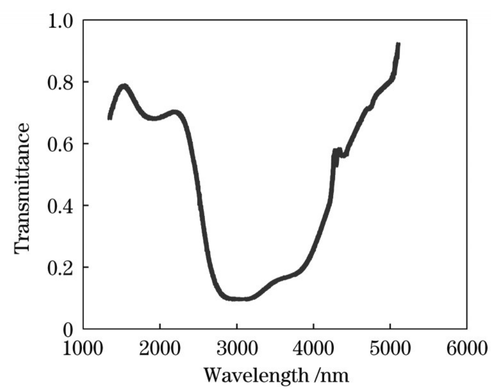

图 2　镀膜后的 Fe:ZnSe 晶体透过率曲线

Fig. 2　Transmittance curve of coated Fe:ZnSe crystal

3　实验结果及讨论

调节 2.8 μm 泵浦激光器功率，当注入到 Fe:ZnSe 晶体中的泵浦功率约为 0.4 W 时，通过光谱仪监测，可以观察到 3.8 μm 附近有激射。此时稍微调大泵浦功率，并采用功率计监测，调节谐振腔使激光器工作在最佳状态。3.8 μm 激光输出功率随注入的泵浦功率的变化如图 3 所示，受限于泵浦源功率，激光器的最大输出功率为 0.97 W，斜率效率为 38.6%。

激光器极限斜率效率（η_{limit}）的计算公式[34]为

$$\eta_{limit}=\eta_{abs}\eta_{quantum}=\left[1-\exp(-\alpha\cdot l)\right]\frac{\lambda_p}{\lambda_s},\qquad(1)$$

式中：η_{abs} 为吸收效率；$\eta_{quantum}$ 为量子效率；α 为吸收系数；l 为晶体长度；λ_p 为泵浦波长；λ_s 为激光波长。实验测量得到晶体的吸收系数 α 为 2.9 cm^{-1}，对应的晶体对泵浦光的吸收效率为 63.8%，取 λ_p～2.8 μm，λ_s～3.8 μm，得到量子效率 $\eta_{quantum}$ 为 73.7%，通过式（1）可以得到极限斜率效率为 47.0%。可见，激光器斜率效率接近其极限斜率效率。通过优化晶体长度，提高泵浦光吸收效率，可以进一步提高激光器斜率效率。另外，从图 3 可以看出，激光器并未出现功率饱和现象，因此，通过继续增加泵浦功率，可以进一步提高输出功率。

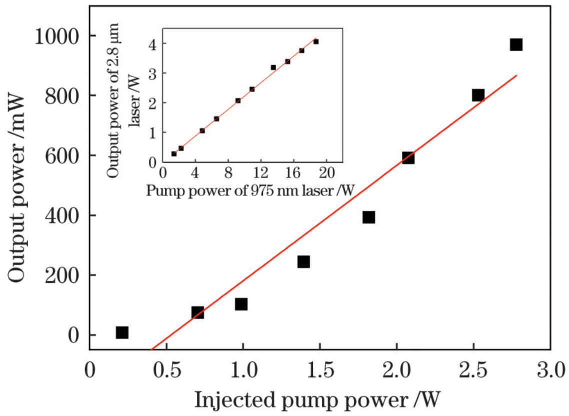

图3　低温下3.8 μm激光的输出功率随注入泵浦功率的变化（插图为2.8 μm激光的输出功率曲线）

Fig. 3　Output power of 3.8 μm laser versus injected pump power at low temperature with output power curve of 2.8 μm laser shown in inset

采用中红外光谱仪（分辨率为0.5 nm）测量了不同输出功率下激光器自由运转时的输出光谱，如图4所示。可以看出，光谱呈现多峰结构，表明谐振腔中有许多纵模参与振荡[27]。随着泵浦功率的增加，中心波长（λ_C）发生红移，从低功率下的3747.1 nm红移至高功率下的3773.3 nm，这是由更高泵浦功率下的局部热效应引起的[27]。同时，光谱谱宽随着泵浦功率的升高而增大，也就是3 dB带宽由低功率下的～4 nm展宽至高功率下的～13 nm。通过测量得到较高功率下的光谱信号背景比（SNR）接近40 dB。采用光栅或棱镜等色散元件作为谐振腔选频元件，可以有效地锁定激光输出波长和压缩激光输出谱宽，目前此项工作正在进行中。

以往报道的自由运转连续波Fe:ZnSe激光器的工作波长均在4 μm以上[25-27]，而本文中激光器的中心波长在3.8 μm附近。Evans[35]研究了Fe:ZnSe晶体在不同温度下的荧光发射谱，其结果如图5所示。可以看出，在低温（<100 K）条件下，荧光谱峰值在3.8 μm附近，与实验结果吻合。另外，谐振腔镀膜曲线的差异也可能是引起激光器自由运转下输出波长不同的原因。从图5还可以看出，随着温度的升高，晶体中的热效应引起的无辐射淬灭作用不断增强，表现为荧光效率不断下降，同时荧光谱峰值发生红移[35]。

长时间运行的激光器的输出功率曲线如图6所示。可以看出，激光器的输出功率比较稳定，计算得到功率不稳定度约为0.4%（均方根值），比非线性频率变换产生连续3.8 μm激光的功率稳定性要高[36]。非线性频率变换方法的转换效率对泵浦功率密度敏感，为了获得较好的转换效率，一般是将泵浦光斑聚焦成非常小的光斑，因此实验室空气气流、聚光系统镜架的长时间漂移以及非线性晶体温度等是引起功率不稳定的重要因素[36]。图6中的插图为3.8 μm激光的远场光斑，可以看出，光斑呈基模高斯分布。

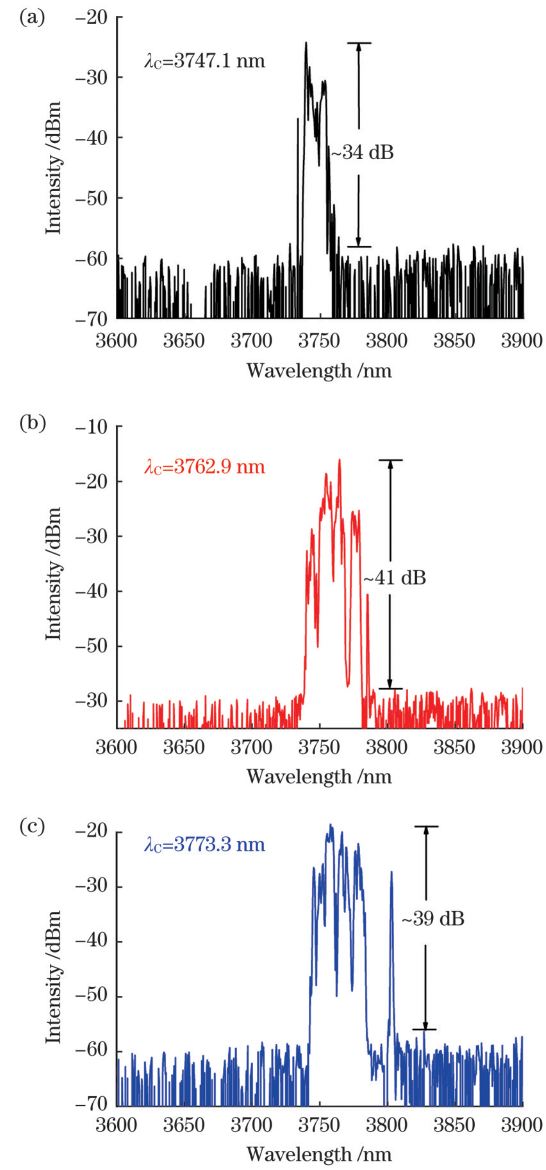

图4　不同输出功率下Fe:ZnSe激光器的输出光谱。（a）74 mW；（b）590 mW；（c）970 mW

Fig. 4　Output spectra of Fe:ZnSe laser at different output powers. (a) 74 mW; (b) 590 mW; (c) 970 mW

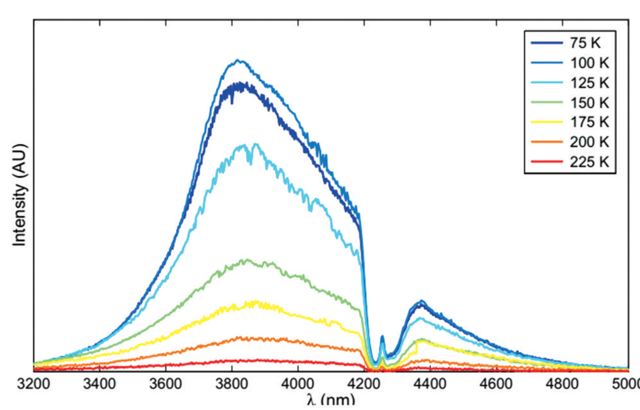

图5　Fe:ZnSe晶体在不同温度下的荧光发射谱[35]

Fig. 5　Fluorescence emission spectra of Fe:ZnSe crystal at different temperatures[35]

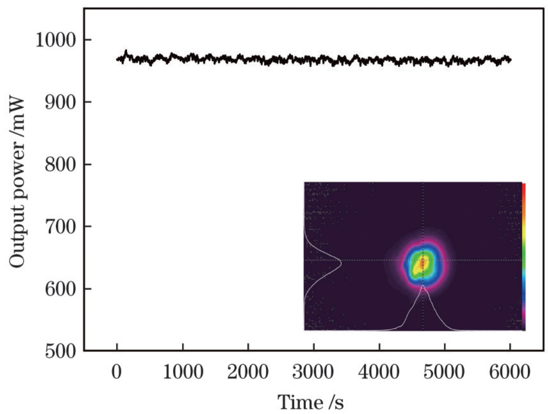

图6 长时间运行的激光器的输出功率曲线(插图为3.8 μm激光的远场光斑)

Fig. 6 Output power curve of long running laser with far-field light spot of 3.8 μm laser shown in inset

4 结 论

利用2.8 μm光纤激光器泵浦Fe:ZnSe晶体,在低温条件下实现了功率达到瓦级的3.8 μm激光连续输出,Fe:ZnSe激光器的最大输出功率为0.97 W,斜率效率为38.6%。通过提升泵浦光纤激光器功率,可以进一步提升激光器的输出功率。

致谢 感谢西北核技术研究所激光与物质相互作用国家重点实验室的栾昆鹏在实验过程中提供了有益的讨论和帮助。

参 考 文 献

[1] Adams J J, Bibeau C, Page R H, et al. 4.0-4.5-μm lasing of Fe: ZnSe below 180 K, a new mid-infrared laser material[J]. Optics Letters, 1999, 24(23): 1720-1722.

[2] 钱传鹏, 余婷, 刘晶, 等. 全固态中波红外激光器研究进展[J]. 现代应用物理, 2020, 11(4): 040102.
Qian C P, Yu T, Liu J, et al. Research progress of all-solid-state mid-infrared laser[J]. Modern Applied Physics, 2020, 11(4): 040102.

[3] 崔宇龙, 周智越, 黄威, 等. 中红外光纤激光技术研究进展与展望[J]. 光学学报, 2022, 42(9): 0900001.
Cui Y L, Zhou Z Y, Huang W, et al. Progress and prospect of mid-infrared fiber laser technology[J]. Acta Optica Sinica, 2022, 42(9): 0900001.

[4] 聂鸿坤, 宁建, 张百涛, 等. 光学超晶格中红外光参量振荡器研究进展[J]. 中国激光, 2021, 48(5): 0501008.
Nie H K, Ning J, Zhang B T, et al. Recent progress of optical-superlattice-based mid-infrared optical parametric oscillators[J]. Chinese Journal of Lasers, 2021, 48(5): 0501008.

[5] Pan Q K, Xie J J, Wang C R, et al. Non-chain pulsed DF laser with an average power of the order of 100 W[J]. Applied Physics B, 2016, 122(7): 200.

[6] Maes F, Fortin V, Bernier M, et al. 5.6 W monolithic fiber laser at 3.55 μm[J]. Optics Letters, 2017, 42(11): 2054-2057.

[7] Maes F, Fortin V, Poulain S, et al. Room-temperature fiber laser at 3.92 μm[J]. Optica, 2018, 5(7): 761-764.

[8] 赵越, 张锦川, 刘传威, 等. 中远红外量子级联激光器研究进展(特邀)[J]. 红外与激光工程, 2018, 47(10): 1003001.
Zhao Y, Zhang J C, Liu C W, et al. Progress in mid-and far-infrared quantum cascade laser(invited) [J]. Infrared and Laser Engineering, 2018, 47(10): 1003001.

[9] Myoung N S, Martyshkin D V, Fedorov V V, et al. Energy scaling of 4.3 μm room temperature Fe: ZnSe laser[J]. Optics Letters, 2011, 36(1): 94-96.

[10] 黄威, 周智越, 崔宇龙, 等. 4.5 W中红外3.1 μm光纤气体激光器[J]. 中国激光, 2022, 49(1): 0101024.
Huang W, Zhou Z Y, Cui Y L, et al. 4.5 W 3.1 μm mid-infrared fiber gas laser[J]. Chinese Journal of Lasers, 2022, 49(1): 0101024.

[11] Koen W, Jacobs C, Bollig C, et al. Optically pumped tunable HBr laser in the mid-infrared region[J]. Optics Letters, 2014, 39(12): 3563-3566.

[12] Cui Y L, Huang W, Wang Z F, et al. 4.3 μm fiber laser in CO_2-filled hollow-core silica fibers[J]. Optica, 2019, 6(8): 951-954.

[13] Murray R T, Runcorn T H, Guha S, et al. High average power parametric wavelength conversion at 3.31-3.48 μm in MgO: PPLN [J]. Optics Express, 2017, 25(6): 6421-6430.

[14] 王菲菲, 聂鸿坤, 刘俊亭, 等. 小型化宽调谐MgO: PPLN中红外纳秒光参量振荡器[J]. 中国激光, 2021, 48(5): 0501015.
Wang F F, Nie H K, Liu J T, et al. Miniaturized widely tunable MgO: PPLN nanosecond optical parametric oscillator[J]. Chinese Journal of Lasers, 2021, 48(5): 0501015.

[15] 郭跃, 常建华, 桂诗信, 等. 连续波中红外差频产生激光光源研究进展[J]. 激光杂志, 2015, 36(12): 8-13.
Guo Y, Chang J H, Gui S X, et al. Progress of continuous-wave mid-infrared laser source based on difference frequency generation [J]. Laser Journal, 2015, 36(12): 8-13.

[16] Bhar G C, Das S, Chatterjee U, et al. Noncritical second harmonic generation of CO_2 laser radiation in mixed chalcopyrite crystal[J]. Applied Physics Letters, 1993, 63(10): 1316-1318.

[17] Frolov M P, Korostelin Y V, Kozlovsky V I, et al. Efficient 10-J pulsed Fe: ZnSe laser at 4100 nm[C] // 2016 International Conference Laser Optics (LO), June 27-July 1, 2016, St. Petersburg, Russia. New York: IEEE Press, 2016: R1-10.

[18] Frolov M P, Korostelin Y V, Kozlovsky V I, et al. High-energy thermoelectrically cooled Fe:ZnSe laser tunable over 3.75-4.82 μm [J]. Optics Letters, 2018, 43(3): 623-626.

[19] Fedorov V, Martyshkin D, Karki K, et al. *Q*-switched and gain-switched Fe: ZnSe lasers tunable over 3.60-5.15 μm[J]. Optics Express, 2019, 27(10): 13934-13941.

[20] Mirov S B, Fedorov V V, Martyshkin D, et al. Progress in mid-IR lasers based on Cr and Fe-doped II-VI chalcogenides[J]. IEEE Journal of Selected Topics in Quantum Electronics, 2015, 21(1): 292-310.

[21] Velikanov S D, Gavrishchuk E M, Zaretsky N A, et al. Repetitively pulsed Fe:ZnSe laser with an average output power of 20 W at room temperature of the polycrystalline active element[J]. Quantum Electronics, 2017, 47(4): 303-307.

[22] Evans J W, Berry P A, Schepler K L. A passively *Q*-switched, CW-pumped Fe: ZnSe laser[J]. IEEE Journal of Quantum Electronics, 2014, 50(3): 204-209.

[23] Uehara H, Tsunai T, Han B Y, et al. 40 kHz, 20 ns acousto-optically *Q*-switched 4 μm Fe: ZnSe laser pumped by a fluoride fiber laser[J]. Optics Letters, 2020, 45(10): 2788-2791.

[24] Pushkin A V, Migal E A, Tokita S, et al. Femtosecond graphene mode-locked Fe:ZnSe laser at 4.4 μm[J]. Optics Letters, 2020, 45(3): 738-741.

[25] Evans J W, Berry P A, Schepler K L. 840 mW continuous-wave Fe:ZnSe laser operating at 4140 nm[J]. Optics Letters, 2012, 37(23): 5021-5023.

[26] Martyshkin D V, Fedorov V V, Mirov M, et al. High power (9.2 W) CW 4.15 μm Fe: ZnSe laser[C]//2017 Conference on Lasers and Electro-Optics (CLEO), May 14-19, 2017, San Jose, CA, USA. New York: IEEE Press, 2017.

[27] Pushkin A V, Migal E A, Uehara H, et al. Compact, highly efficient, 2.1-W continuous-wave mid-infrared Fe: ZnSe coherent source, pumped by an Er: ZBLAN fiber laser[J]. Optics Letters, 2018, 43(24): 5941-5944.

[28] 孔心怡, 柯常军, 胡呈峰, 等. 65 mJ室温Fe^{2+}:ZnSe中红外激光器[J]. 中国激光, 2018, 45(1): 0101011.
Kong X Y, Ke C J, Hu C F, et al. 65 mJ Fe^{2+}:ZnSe mid-infrared laser at room temperature[J]. Chinese Journal of Lasers, 2018, 45(1): 0101011.

[29] Li Y Y, Yang K, Liu G Y, et al. A 1 kHz Fe:ZnSe laser gain-switched by a $ZnGeP_2$ optical parametric oscillator at 77 K[J]. Chinese Physics Letters, 2019, 36(7): 074201.

[30] Li Y Y, Dai T Y, Duan X M, et al. Fe:ZnSe laser pumped by a 2.93-μm Cr, Er: YAG laser[J]. Chinese Physics B, 2019, 28(6): 064203.

[31] Pan Q K, Xie J J, Chen F, et al. Transversal parasitic oscillation suppression in high gain pulsed Fe^{2+} : ZnSe laser at room temperature[J]. Optics & Laser Technology, 2020, 127: 106151.

[32] 沈炎龙, 黄珂, 周松青, 等. 10 W级高效率单模中红外2.8 μm光纤激光器[J]. 中国激光, 2015, 42(5): 0502008.
Shen Y L, Huang K, Zhou S Q, et al. 10 W-level high efficiency single-mode mid-infrared 2.8 μm fiber laser[J]. Chinese Journal of Lasers, 2015, 42(5): 0502008.

[33] Voronov A A, Kozlovskii V I, Korostelin Y V, et al. A continuous-wave Fe^{2+}: ZnSe laser[J]. Quantum Electronics, 2008, 38(12): 1113-1116.

[34] Evans J W, Sanamyan T, Berry P A. A continuous wave Fe: ZnSe laser pumped by efficient Er: Y_2O_3 laser[J]. Proceedings of SPIE, 2015, 9342: 93420F.

[35] Evans J W. Iron-doped zinc selenide: spectroscopy and laser development[D]. Maxwell AFB: Air University, 2014.

[36] Zhao J Q, Yao B Q, Tian Y, et al. High power, continuous wave, singly resonant OPO based on MgO: PPLN[J]. Laser Physics, 2010, 20(10): 1902-1906.

3.8 μm Continuous-Wave All Solid-State Fe:ZnSe Laser

Shen Yanlong*, Wan Yingchao, Wang Yousheng, Li Gaopeng, Ma Lianying, Chai Tongxin, Chen Zhengge, Zhu Feng, Huang Ke, Feng Guobin

State Key Laboratory of Laser Interaction with Matter, Northwest Institute of Nuclear Technology, Xi'an 710024, *Shaanxi, China*

Abstract

Objective There are increasing demands for mid-infrared lasers at 3–5 μm, which overlaps with the transparency window of atmosphere, for their potential applications in various fields, including laser surgery, spectroscopy, infrared countermeasures, environmental monitoring, and laser communication. There are lots of approaches to achieve lasers at 3–5 μm band, which can be roughly divided into two major categories. The first category is based on population inversion, namely the linear method, which includes HF/DF gas lasers, semiconductor cascade lasers, fiber lasers, and solid-state lasers (typically Fe:ZnSe or Fe:ZnS lasers). The second category is based on the nonlinear effect, including optical parametric oscillators (OPO, typically using PPLN and ZGP crystals as nonlinear media), difference frequency generation (DFG), and frequency doubling. Compared to these lasers, the Fe:ZnSe or Fe:ZnS lasers, emitting at the mid-infrared range of 4–5 μm, enjoy several advantages, including high efficiency, wide wavelength-tuning range, and compactness of optical cavity. As a consequence, lots of efforts have been made in the development of Fe:ZnSe/Fe:ZnS lasers in the past decade. For some practical applications, continuous-wave (CW) Fe:ZnSe/Fe:ZnS lasers are required. Several CW Fe:ZnSe lasers, all of which operates at the wavelengths of over 4 μm, have been demonstrated by using various CW pumping sources, including the Cr:ZnSe laser, Er:YAG laser, Er:ZBLAN fiber laser, and Er:Y_2O_3 laser. Limited by matured pump sources at ~3 μm, CW Fe:ZnSe lasers were seldom domestically reported. In this paper, a CW Fe:ZnSe laser at ~4 μm is demonstrated by using a self-developed continuous-wave Er-doped fiber laser at 2.8 μm.

Methods The pump source used in our study is a continuous-wave Er-doped fiber laser at ~2.8 μm developed in our lab. It has a maximum output power of about 4 W. The gain medium, i. e. , the Fe:ZnSe crystal is 3.5 mm in length and has a cross section of 10 mm×10 mm, with the Fe^{2+} ion concentration of 1.0×10^{19} cm^{-3}. For obtaining effective CW lasing, the crystal is wrapped in a piece of indium foil and clamped to a copper mount cooled to ~77 K by liquid nitrogen in a cryostat, owing to the lifetime of the upper laser level in a Fe:ZnSe crystal being as short as 370 ns at room temperature while around 57 μs at 77 K. Longer lifetime of upper laser level makes continuous-wave emission much easier. The faces of the gain crystal are anti-reflection coated at 2.7–4.8 μm. Windows of the cryostat are 3 mm CaF_2 plates with AR coated at 2.7–4.8 μm. In the laser cavity arrangement, the feedback is a special coated CaF_2 plano-concave mirror, while the output mirror is another CaF_2 plano-concave mirror with a coupling ratio of ~35%. The radius of each cavity mirror is identical at 50 mm. A dichroic mirror is placed with an incidence angle of ~45° to separate the pump beam and output laser beam. An uncoated CaF_2 lens with a focal length of 50 mm is used to couple the pump beam into the crystal. Unlike the previous demonstrations of CW Fe:ZnSe lasers, the pump direction in our experiment is counter-pumping, i. e. , the pump beam and laser beam propagate in opposite directions.

Results and Discussions An optical spectrum analyzer is used to monitor the lasing of the 4 μm signal. When the pump power is increased to about 0.4 W, there is a little peak in captured spectrum. Subsequently, fixing the pump power slightly higher than the threshold, we adjust the cavity mirrors and the coupling lens to maximize the output power. The output power as a function of pump power is recorded and shown in Fig. 3. The maximum power is 0.97 W, which is limited by the pump capability. The slope efficiency is fitted to be ~38.6%, which nearly approaches the limited efficiency of the current laser. The measured laser spectra are shown in Fig. 4. The central wavelength shifts from 3747.1 nm at low output power to 3773.3 nm at high output power with a signal to noise ratio (SNR) of as high as 40 dB, which is also named with "red-shift" and is common in free-running solid-state lasers. The wavelength in this laser is approximately 3.8 μm. The laser spot indicates that the beam profile has a desirable fundamental Gaussian distribution.

Conclusion A watt-level high efficiency 3.8 μm mid-infrared all-solid-state continuous wave laser is demonstrated in this study. The output power of 0.97 W with a central wavelength at 3.8 μm with a slope efficiency of 38.6% from Fe:ZnSe crystal is obtained by employing a self-developed continuous-wave Er-doped fiber laser at 2.8 μm as the pump source. The pump source is employed under liquid nitrogen cooling, and the beam profile has a desirable fundamental Gaussian distribution.

Key words lasers; all solid-state lasers; mid-infrared laser; Fe:ZnSe crystal; high efficiency